



This open access document is published as a preprint in the Beilstein Archives with doi: 10.3762/bxiv.2019.52.v1 and is considered to be an early communication for feedback before peer review. Before citing this document, please check if a final, peer-reviewed version has been published in the Beilstein Journal of Nanotechnology.

This document is not formatted, has not undergone copyediting or typesetting, and may contain errors, unsubstantiated scientific claims or preliminary data.

Preprint Title The impact of crystal size and temperature on the adsorption-induced flexibility of the Zr-based metal-organic framework DUT-98

Authors Simon Krause, Volodymyr Bon, Hongchu Du, Rafal E. Dunin-Borkowski, Ulrich Stoeck, Irena Senkowska and Stefan Kaskel

Article Type Full Research Paper

Supporting Information File 1 ESI.pdf; 2.0 MB

ORCID® iDs Simon Krause - <https://orcid.org/0000-0001-9504-8514>; Volodymyr Bon - <https://orcid.org/0000-0002-9851-5031>; Hongchu Du - <https://orcid.org/0000-0002-4661-4644>; Rafal E. Dunin-Borkowski - <https://orcid.org/0000-0001-8082-0647>; Irena Senkowska - <https://orcid.org/0000-0001-7052-1029>

License and Terms: This document is copyright 2019 the Author(s); licensee Beilstein-Institut.

This is an open access publication under the terms of the Creative Commons Attribution License (<http://creativecommons.org/licenses/by/4.0>). Please note that the reuse, redistribution and reproduction in particular requires that the author(s) and source are credited.

The license is subject to the Beilstein Archives terms and conditions: <https://www.beilstein-archives.org/xiv/terms>.

The definitive version of this work can be found at: doi: <https://doi.org/10.3762/bxiv.2019.52.v1>

The impact of crystal size and temperature on the adsorption-induced flexibility of the Zr-based metal-organic framework DUT-98

Simon Krause^{1,2*}, Volodymyr Bon¹, Hongchu Du^{3,4}, Rafal E. Dunin-Borkowski³, Ulrich Stoeckl¹, Irena Senkowska¹, Stefan Kaskel^{1*}

* correspondence to Simon Krause: simon.krause@rug.nl , Stefan Kaskel: Stefan.kaskel@tu-dresden.de

Affiliations:

1) Department of Inorganic Chemistry, Technische Universität Dresden, Bergstrasse 66, 01062 Dresden, Germany

2) Centre for Systems Chemistry, Stratingh Institute for Chemistry, University of Groningen, Nijenborgh 4, 9747 AG Groningen, The Netherlands

3) Ernst Ruska-Centre for Microscopy and Spectroscopy with Electrons, Forschungszentrum Juelich GmbH, 52425 Juelich, Germany

4) Central Facility for Electron Microscopy (GFE), RWTH Aachen University, 52074 Aachen, Germany

Abstract:

In this contribution we analyse the influence of adsorption cycling, crystal size, and temperature on the switching behaviour of the flexible Zr-based metal-organic framework DUT-98. We observe a shift in the gate opening pressure upon cycling of adsorption experiments of micro meter-sized crystals and assign this to a fragmentation of the crystals. In a series of modulated syntheses we downsize the average crystal size of DUT-98 crystals from 120 μm to 50 nm and characterize the obtained solids by X-ray diffraction, infrared spectroscopy, as well as scanning and transmission electron microscopy. We analyse the adsorption behaviour by nitrogen and water adsorption at 77 K and 298 K, respectively and show that adsorption-induced flexibility is only observed for micro meter-sized crystals. Nanometer-sized crystals were found to exhibit reversible type I adsorption behaviour upon adsorption of nitrogen and exhibit a crystal-size dependent steep water uptake of up to 20 mmol g^{-1} at 0.5 p/p_0 with potential for water harvesting and heat pump applications. We furthermore investigate the temperature-induced structural transition by *in situ* PXRD. At temperatures beyond 110 °C the open pore state of nano meter-sized DUT-98 crystals are found to irreversibly transform in a closed pore state. The connection of crystal fragmentation upon adsorption cycling and the crystal size-dependence of the adsorption-induced flexibility is an important finding for evaluation of these materials in future adsorption-based applications. This work thus extends the limited amount of studies on crystal size effects in flexible MOFs and hopefully motivates further investigations into this field.

Keywords: crystal engineering, flexible metal-organic frameworks, water adsorption, crystal size

Introduction:

In the past 20 years, research in the area of metal-organic frameworks (MOFs) has brought up various record holding materials in terms of surface area¹ and gas storage² but also given rise to unprecedented adsorption phenomena³ often associated to structural transitions. An increasing number of the so-called flexible MOFs are being reported and their use in the areas of storage⁴, separation⁵ and sensing⁶ of gases are being evaluated and their structural flexibility and adsorption behavior can be manipulated by applying chemical functionalization to the ligand⁷ and metal cluster⁸. However, recent examples progressively illustrate the manipulation of adsorption properties of switching adsorbents by variation of size⁹⁻¹³ and morphology¹⁴ of the crystals, without changing the composition of the MOF. Reports on MIL-53 indicate an impact of crystal morphology and size on the structural contraction upon solvent removal^{15,16}. In a recent report, we demonstrated the suppression of adsorption-induced contraction in DUT-49 (DUT-Dresden University of Technology) upon downsizing of the crystals below 1 μm ⁹ and loss of flexibility upon downsizing of DUT-8 crystals^{17,18}. In a similar fashion suppression of gate opening in ZIF-8 upon crystal downsizing was reported¹⁰⁻¹³ and Kitagawa and co-worker reported on a shape-memory effect of gate opening transitions upon crystal downsizing in a pillared-layer MOF.¹⁹ Although these reports demonstrate the influence of crystal size on the structural behavior of flexible MOFs, the materials for which this phenomena were reported differ in terms of topology, the nature of the structural transitions and the resulting adsorption behavior. In fact, it appears to be possible that some reported non-flexible MOFs can exhibit flexibility if their crystals are synthesized in a specific size or morphology or vice versa: It is thus of crucial importance to extend investigations on crystal size effects in flexible and non-flexible MOFs to further define these phenomena and potentially postulate a global mechanism.

Results and Discussion:

In this contribution we report on the impact of crystal size on adsorption- and temperature-induced structural transitions of DUT-98, a flexible Zr-based MOF. The structure of DUT-98 comprises of 1D supermolecular building chains (SBC) which consist of Zr₆-cluster interconnected by 3,6-carbazole dicarboxylate ligands²⁰. An additional benzoate functionality of the ligand connects the SBC into a 3D framework with a structure (Figure 2) similar to MIL-53^{21,22}.

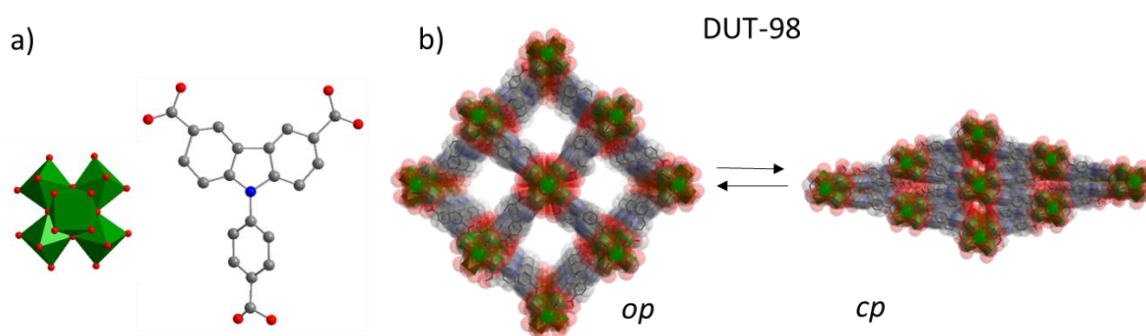


Figure 1. a) Zr-oxo cluster (green) and organic ligand CPCDC = 9-(4-carboxyphenyl)-9H-carbazole-3,6-dicarboxylate) applied in the construction of DUT-98; b) crystal structure transformation of DUT-98 open pore (op) to closed pore (cp).

Upon removal of the solvent molecules from the pore-channels by supercritical activation, the wine-rack type channels of DUT-98 are contracted almost completely reducing the gas

accessible pore volume by 98%. By adsorption of various guest molecules including N₂ (at 77 K), CO₂ (at 195 K), *n*-butane (at 273 K), and various alcohols (at 298 K) DUT-98_{cp} (*cp* = closed pore) reopens the pores at defined gate opening pressures (p_{go}) giving rise to isotherms with distinct steps, typical for gate opening MOFs. Upon cyclic adsorption/desorption, the structural transition and the corresponding *op* and *cp* phase remains unchanged (Supplementary Figure 3) however a shift of p_{go} towards lower pressures is observed, indicating that the material properties change upon adsorption and desorption of various gases and vapors.

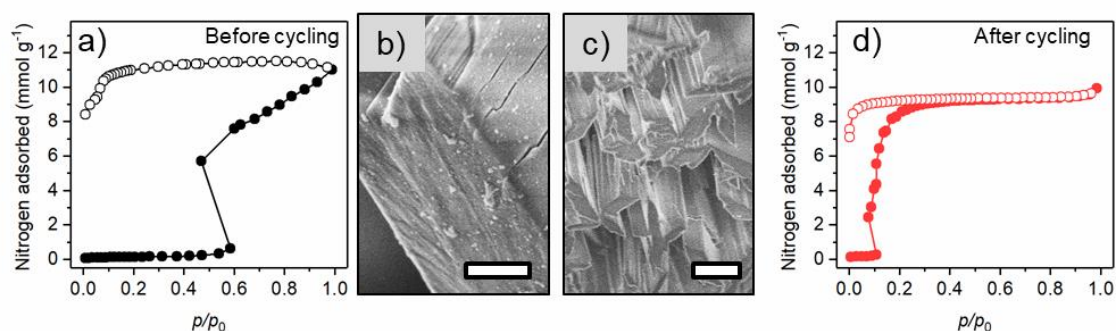


Figure 2. Nitrogen adsorption isotherms at 77 K (a,d) and SEM images (scale bars 1 μ m) (b,c) of DUT-98(1) before (a,b) and after (c,d) adsorption experiments with nitrogen, CO₂, *n*-butane, and vapors of alcohols and hydrocarbons (for details on the adsorption experiments see reference²³). Closed symbols: adsorption, open symbols: desorption.

Only a few reports on cycling behavior of flexible MOFs can be found in the literature. Shi *et al.* reported on a shift of the gate pressure towards higher pressures upon cycling of nitrogen adsorption at 77 K in Zn₂(tdc)₂(pvq)] (H₂tdc = 2,5-thiophenedicarboxylic acid, pvq = 5-(2-(pyridin-4-yl)vinyl)quinoline)²⁴. Similar results are reported by Su *et al.* on a redox active flexible MOF²⁵. Nitrogen isotherms at 77 K of both materials show a pronounced pressure reduction upon structural opening referred to by the authors as “negative gas pressure”. Such artificial pressure reduction upon structural expansion is also observed in DUT-98 and a few other examples in the literature^{23,25-27} and is a clear indication for a metastable adsorption state as previously described by Kitagawa and co-workers²⁸.

In a previous work we addressed changes of adsorption behavior in flexible MOFs upon cycled *n*-butane adsorption experiments on a series of flexible MOFs with predominantly one-dimensional channels²⁹. In that investigation p_{go} in isotherms of DUT-8 and SNU-9 was found to be shifted to higher pressures upon cycling. In contrast, cycling of MIL-53 and ELM-11 were found to only slightly impact the adsorption behavior. Analysis of the SNU-9 and DUT-8 crystals before and after cycling showed deformation and fragmentation of the relatively large crystal compared to the microcrystals of MIL-53 and ELM-11 which were not affected by the cycling. This indicates that larger crystals are more prone to undergo deformation and fragmentation upon repeated contraction/expansion due to the higher number of unit cells merged in a single crystal that have to collectively switch upon structural transition. However, in all reported cases p_{go} was shifted to higher pressures upon cycling in contrast to DUT-98, for which the gate pressure is found to be shifted to lower pressures. SEM images of the crystals of DUT-98 before and after cycling (Supplementary Figure 1, Supplementary Figure 2, Figure 2) show that the rod-shaped crystals of DUT-98_{cp} are fragmented into smaller needle-like pieces.

Structurally, this indicates a fragmentation along the pore channels, which run along the rods and crystallographic b -axis in DUT-98 cp . Thus, bond cleavage upon fragmentation is expected to occur at the edges of the SBC in DUT-98, which run in parallel to the pore channels. This fragmentation is likely caused by the stress upon structural reopening during adsorption and contraction during desorption in which the unit cell volume changes by over 140%. The change in the adsorption isotherm as well as the crystal morphology and fragmentation indicate that the adsorption behavior depends on the size of the crystal domains. The question is whether this behavior can also be observed if the crystals were initially synthesized smaller in size?

Recently it has been shown that the crystal size of Zr-based MOFs can easily be controlled by adding acidic modulators^{30,31} or water^{32,33} to the reaction mixture in the solvothermal synthesis, which increase or decrease the crystal size, respectively. By changing the solvent, reaction time, concentration of acetic acid, and water content of the reaction mixture, four DUT-98 samples containing particles of different size, namely DUT-98(1) – (4) could be obtained (Figure 3).

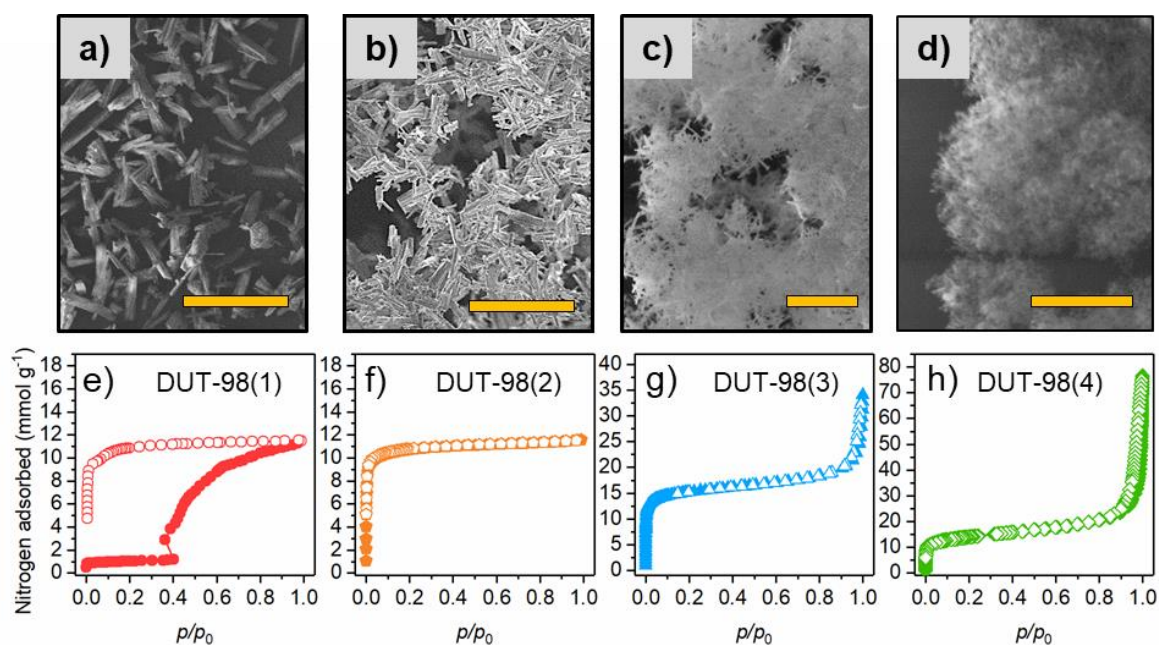


Figure 3. a-d) SEM images and e-h) nitrogen adsorption isotherms at 77 K of DUT-98(1) (a,e), DUT-98(2) (b,f), DUT-98(3) (c,g), and DUT-98(4) (d,h), Scale bars a) 200 μm, b) 50 μm, c) 1 μm, and d) 500 nm. Closed symbols: adsorption, open symbols: desorption.

All solvated samples were analyzed by powder X-ray diffraction (PXRD) proving the phase purity of the desired DUT-98 op (open pore) phase (Figure 4). Significant peak broadening is observed for samples 3 and 4, which is indicative for the presence of nanometer sized crystals. The samples were further activated according to the procedure previously reported for DUT-98(1)²⁰. Solvent free white powders and in the case of DUT-98(4) low-density monolithic structures (similar to aerogels recently reported for gel-like Zr MOFs^{34,35}) were obtained. SEM analysis shows the rod-like crystal morphology with crystal length in the range of 120 μm for DUT-98(1), of 10 μm for DUT-98(2), of 500 nm for DUT-98(3), and 50 nm for DUT-98(4). Thermogravimetric analysis of activated DUT-98 samples shows a decrease in decomposition temperature from 440 - 420 °C with decreasing crystal size (Supplementary Figure 11). However, the general shape of the TGA-curves is very similar pointing to the phase purity of

the powders. PXRD analysis of the supercritically activated samples shows again peak broadening upon downsizing. However, for DUT-98(1) – (3) samples, a shift of reflection positions and appearance of new peaks, different from that of the *op* phase are observed (Figure 4) which was previously assigned to the contraction of DUT-98*op* into DUT-98*cp*.

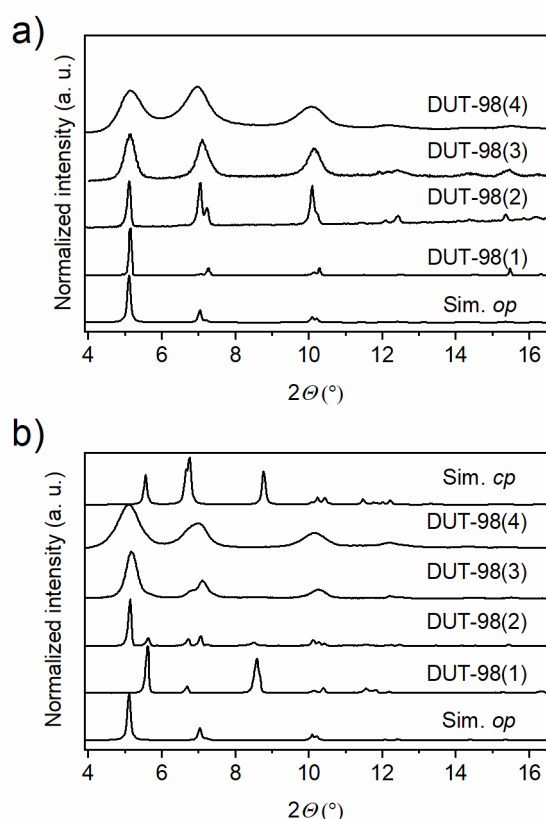


Figure 4. PXRD Patterns of DUT-98 with different crystal size a) as made and b) activated by supercritical solvent removal.

Interestingly, only DUT-98(1) exhibits complete contraction of the whole bulk, while the other three samples only exhibit peaks of low intensity of the DUT-98*cp* phase and primarily remaining peaks of the *op* phase. Consequently, in the samples with smaller crystals, the majority of crystals or crystal domains remain in the *op* phase and only part of the sample undergoes contraction upon solvent removal by supercritical activation. A quantitative phase analysis of the *op-cp* mixture by Rietveld refinement was not possible due to the anisotropy of the crystals and the large peak broadening, leading to an overlap of the reflections of the two phases. To further analyze the nature of the phase mixture we aimed to perform high resolution transmission electron microscopy (HRTEM) analysis on DUT-98(4) a technique previously applied in the microscopic analysis of defects in Zr-MOFs³⁶. Unfortunately, the nanocrystals of DUT-98(3) decomposed during the measurement. By reproducing the synthesis using Hf instead of Zr we obtained DUT-98(Hf) with a crystal length of 130 nm which demonstrated the same structure as shown by PXRD (Supplementary Figure 9). Interestingly, DUT-98(Hf) showed enhanced stability towards the electron beam allowing for detail microscopic analysis of the nanocrystals and their structure. HRTEM analysis shows uniform pore channels along the rod shaped nano-crystals with a spacing of the Hf-cluster of 1.5 nm, which is in good agreement to the lattice parameter and the inter-cluster distance of the DUT-98*op* crystal structure (Supplementary Figure 8). The regular arrangement of the clusters

indicates a high symmetry which matches the tetragonal symmetry in DUT-98 op . In contrast, the DUT-98 cp phase would exhibit a different microscopic structure due to the lower, monoclinic symmetry. In addition, no missing cluster or linker defects could be detected which are well known for Zr-MOFs^{36,37} demonstrating that the observed behavior does not depend on increasing concentration of lattice defects. Thus, all investigated DUT-98(Hf) crystals exhibit a structure expected for the open phase, which supports the results obtained from PXRD and nitrogen adsorption at 77 K in which the op phase is the dominant phase. We thus derive that the presence of the cp phase is based on a physical mixture of crystals exhibiting either op or cp phase and these phases do not co-exist as domains within a single crystal. This supports the assumption that structural contraction is a cooperative phenomenon that propagates through the whole crystal. To further analyze the porosity and adsorption-induced flexibility, N₂ adsorption isotherms at 77 K were recorded on DUT-98(2) – (4) and compared to the initial isotherm of DUT-98(1).

Interestingly, only DUT-98(1) exhibits flexible behavior evident by the stepped isotherm and wide hysteresis. DUT-98(2) exhibits type I behavior reflecting the microporosity of the MOF. DUT-98(3) and (4) show type I at lower and type IV behavior at high relative pressures, reflecting the microporous nature of the MOF and additional interparticular mesoporosity, respectively. This is well reflected when comparing the specific micropore volume and specific BET surface area (Supplementary Table 2) of DUT-98(2)-(4) which exhibit comparable values with DUT-98(3) showing the highest values of 0.53 cm³ g⁻¹ and 1303 m² g⁻¹, respectively. Interestingly, neither of the materials reach the pore volume value calculated theoretically from the crystal structure of DUT-98 op , indicating that the cp fraction observed in the PXRD patterns does not reopen upon adsorption of nitrogen at 77 K. In this regard, DUT-98(Hf) is found to exhibit similar adsorption properties (Supplementary Figure 10) compared to DUT-98(3) which further supports the observations made by PXRD and HRTEM. In fact, neither of the isotherms of DUT-98(Hf) nor DUT-98(2)-(4) show any indication of adsorption-induced flexible behavior, evident by steps or hysteresis in the isotherm. Thus, nitrogen, known to be a rather weakly interacting adsorbate cannot initiate a structural contraction in downsized crystals of DUT-98.

The contraction mechanism in DUT-98(1) was previously shown to depend on pore shrinkage along a reorganization of water molecules within the structure close to the Zr-cluster²³. The Diffuse Reflectance Fourier transform (DRIFT) spectroscopy shows typical vibrations corresponding to the linker and OH groups of the MOFs in all materials (Supplementary Figure 12). To analyze whether adsorption of water can promote contraction in small crystals of DUT-98 op , water adsorption experiments were conducted at 298 K for DUT-98(2) - (4).

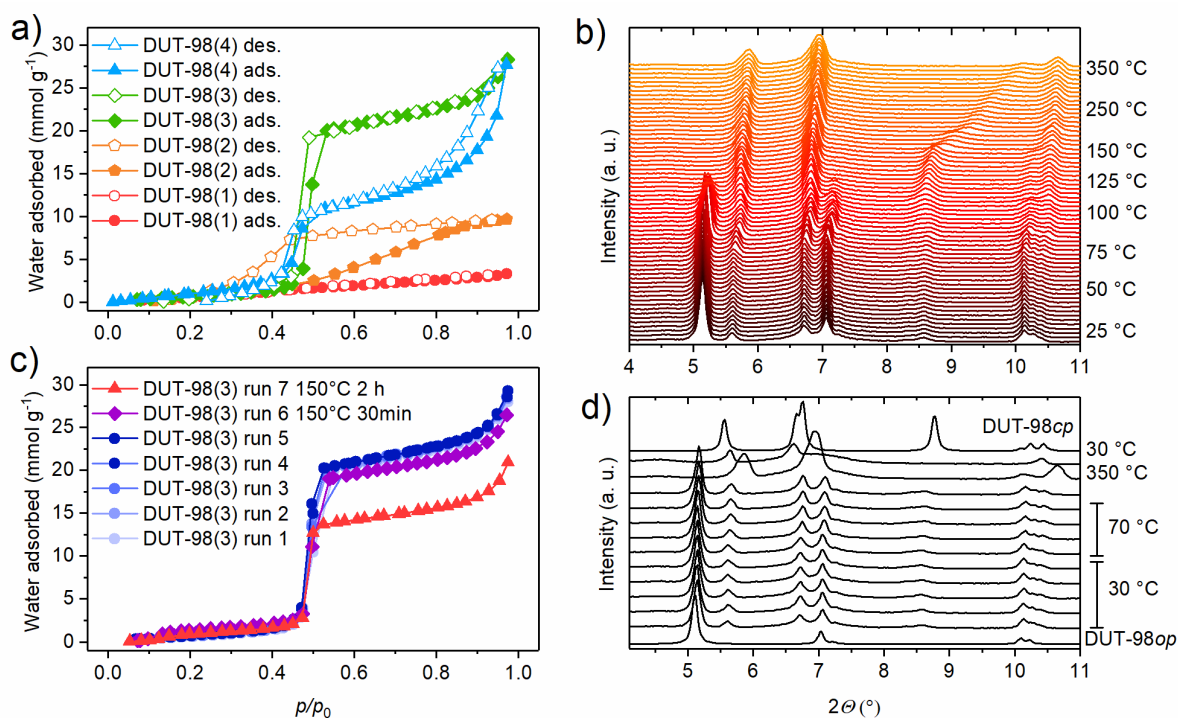


Figure 5. a) Water physisorption experiments at 298 K on: a) DUT-98(1)-(4) and c) DUT-98(3) after cycling and after thermal treatment. (Filled symbols: adsorption, open symbols: desorption). *In situ* temperature variable PXRD of: b) DUT-98(2) and d) DUT-98(2) cycled at lower temperature.

In DUT-98(1), no significant adsorption of water can be observed indicating that structural opening cannot be induced *via* water adsorption. In DUT-98(2) on the other hand, an increase in uptake is observed around relative pressure of 0.5, indicating increased adsorption ability. In contrast to other Zr-based MOFs³⁸ this is rather high relative pressure for water adsorption, indicating a hydrophobic character of the pore inner surface. In DUT-98(3) a steep increase in water adsorption is observed again at around relative pressure of 0.5, however the uptake is found to be almost 3 times higher compared to DUT-98(2). DUT-98(4) exhibits the same steep increase but a wide hysteresis at higher pressure indicating the dominant contribution of interparticular mesoporosity over the microporosity of the pore channels. Repeated water adsorption experiments on DUT-98(3) show near identical isotherms supporting the absence of structural transitions and cycling stability under these conditions. The high cycling stability and steep uptake at a relative pressure around p/p_0 0.5 might make this material an interesting candidate for water capture applications.³⁹⁻⁴¹

In the original report on DUT-98 an irreversible contraction of the pores upon thermal activation at 80°C in vacuum was described. An unknown structural transition different from the contraction to DUT-98 $_{cp}$ takes place and the formation of a high temperature (DUT-98 $_{ht}$) phase was proposed. Although the structure of this phase could not be refined from PXRD and single crystal diffraction data, the obtained PXRD patterns were found to be very similar to the cp phase and DRIFT analysis indicates that the transition is supported by the loss of lattice water molecules⁴². Because the crystal downsizing allows for the preservation of the desolvated DUT-98 $_{op}$ phase, we investigated the impact of elevated temperatures on

structural transition in DUT-98 op via *in situ* variable temperature PXRD. The experiments were conducted under vacuum on supercritically activated DUT-98(2) in the temperature range of 30 - 350 °C. These conditions are often used for thermal activation of MOFs and were previously applied on the analysis of DUT-98(1)²³. In the range of 30 - 75 °C no change in the PXRD patterns could be observed and the material could be heated and cold down within this range without any indication of structural changes (Figure 5). However, upon further heating, a clear increase in peak intensity assigned to reflections of DUT-98 ht is observed. Around 100 °C, peaks of the op phase disappear and a phase pure ht phase is obtained. At temperatures beyond 150 °C, peaks at 8.5 and 11.5°, respectively, exhibit a gradual shift towards higher diffraction angle, indicating a reduction of the lateral inter-cluster distance. This would support the proposed enhanced contraction upon heating potentially supported by the loss of lattice water not evident in the DRIFT spectra after heating (Supplementary Figure 13). Such a ht phase has also been observed for MIL-53, which corresponds to the loss of water from the structure. Attempts to index the obtained patterns failed potentially due to a change in symmetry and the high crystal anisotropy. Nevertheless, the variable temperature PXRD analysis clearly shows that elevated temperatures initiate an irreversible structural transition in DUT-98(2) which was also previously observed for DUT-98(1)²⁰. This is well reflected by water adsorption experiments carried out on DUT-98(3) in which the uptake is found to decrease upon heating of the powder at 80 °C in dynamic vacuum (Figure 5c). Although no adsorption induced transitions could be observed in downsized DUT-98 crystals, the samples showed a high sensitivity towards elevated temperature in vacuum, conditions found to initiate an irreversible structural contraction. This finding implicates that guest free DUT-98 op is a metastable phase and DUT-98 cp is the thermodynamic stable phases observed upon solvent removal in DUT-98(1) and in parts in DUT-98(2)-(4). Thus, smaller crystal sizes seem to stabilize the presence of a metastable op phase by impacting the activation barrier, presumably due to contribution of the surface energy and other factors. This observation was previously made for DUT-8 for which the guest free metastable op phase was also found to be stabilized upon crystal downsizing. Reports on shape memory effects^{19,43} in flexible MOFs found to be intrinsically connected to the formation of metastable states indicate that crystal size and morphology are in fact parameters that significantly alter the free energy landscape of bistable adsorbents and therefore also impact the adsorption behavior.

Conclusion

In conclusion we demonstrated that the adsorption behavior and structural transition of the flexible Zr-MOF DUT-98 strongly depends on the size of the crystals. In addition, we demonstrate that cycled adsorption experiments can have a large impact on the properties of flexible MOFs by altering the crystal morphology, size and mosaicity. In many regards DUT-98 is found to behave similar to DUT-8 and the applied methods indicate changes of the activation energies upon crystal downsizing to be responsible for the observed behavior. The lack of adsorption-induced structural transition for nanometer-sized crystals was previously described also in ZIF-8¹³ and DUT-49⁹. However, the mechanism and structural transitions in these flexible MOFs are of a different nature and make a mechanistic comparison with DUT-98 difficult. After all, there might not be a single theory for explaining the effects of crystal size variation on the adsorption behavior of flexible MOFs. Only further crystal size-depending analysis of novel flexible MOFs with different transition and structures can solidify the presented observations and help to postulate a detailed mechanism. Furthermore, the effect

of microscopic defects upon changes in the synthesis procedure should not be neglected as increasing numbers of defects have been demonstrated to strongly alter the mechanical stability of MOFs.⁴⁴⁻⁴⁶ In accordance, novel experimental investigations on flexible MOFs should consider crystal size and cycling effects and include these in experiments and discussion. In addition, we would like to motivate computational chemists to extend recent efforts⁴⁷ in developing strategies to analyze these phenomena *in silico*.

Acknowledgements:

The authors would like to thank Annika Leifert for SEM analysis. Simon Krause would like to thank the Alexander von Humboldt-Foundation for funding. Hongchu Du acknowledges the support from the Deutsche Forschungsgemeinschaft (DFG) under Grant SFB 917 Nanoswitches and under the core facilities Grant MA 1280/40-1. Stefan Kaskel acknowledges the support from DFG under Grant FOR 2433.

Supporting Information:

Synthetic procedures and additional characterization of the discussed compounds can be obtained from the Electronic Supporting Information.

Conflict of interest:

The authors declare no conflict of interest.

References

- 1 Hönicke, I. M.; Senkovska, I.; Bon, V.; Baburin, I. A.; Bönisch, N.; Raschke, S.; Evans, J. D. Kaskel, S. *Angew. Chem. Int. Ed.*, **2018**, *57*, 13780-13783. doi:10.1002/anie.201808240
- 2 Li, H.; Wang, K.; Sun, Y.; Lollar, C. T.; Li, J.; Zhou, H.-C. *Mater. Today*, **2018**, *21*, 108-121. doi:10.1016/j.mattod.2017.07.006
- 3 Krause, S.; Bon, V.; Senkovska, I.; Stoeck, U.; Wallacher, D.; Többens, D. M.; Zander, S.; Pillai, R. S.; Maurin, G.; Coudert, F. o.-X. Kaskel, S. *Nature*, **2016**, *532*, 348-352. doi:10.1038/nature17430
- 4 Mason, J. A.; Oktawiec, J.; Taylor, M. K.; Hudson, M. R.; Rodriguez, J.; Bachman, J. E.; Gonzalez, M. I.; Cervellino, A.; Guagliardi, A.; Brown, C. M.; Llewellyn, P. L.; Masciocchi, N. Long, J. R. *Nature*, **2015**, *527*, 357. doi:10.1038/nature15732
- 5 Chang, Z.; Yang, D.-H.; Xu, J.; Hu, T.-L.; Bu, X.-H. *Adv. Mater.*, **2015**, *27*, 5432-5441. doi:10.1002/adma.201501523
- 6 Zhang, X.; Zhang, Q.; Yue, D.; Zhang, J.; Wang, J.; Li, B.; Yang, Y.; Cui, Y. Qian, G. *Small*, **2018**, *14*, 1801563. doi:10.1002/sml.201801563
- 7 Biswas, S.; Ahnfeldt, T.; Stock, N. *Inorg. Chem.*, **2011**, *50*, 9518-9526. doi:10.1021/ic201219g
- 8 Yot, P. G.; Yang, K.; Guillerm, V.; Ragon, F.; Dmitriev, V.; Parisiades, P.; Elkaïm, E.; Devic, T.; Horcajada, P.; Serre, C.; Stock, N.; Mowat, J. P. S.; Wright, P. A.; Férey, G. Maurin, G. *Eur. J. Inorg. Chem.*, **2016**, *2016*, 4424-4429. doi:10.1002/ejic.201600263
- 9 Krause, S.; Bon, V.; Senkovska, I.; Többens, D. M.; Wallacher, D.; Pillai, R. S.; Maurin, G. Kaskel, S. *Nat. Commun.*, **2018**, *9*, 1573. doi:10.1038/s41467-018-03979-2
- 10 Tanaka, H.; Ohsaki, S.; Hiraide, S.; Yamamoto, D.; Watanabe, S. Miyahara, M. T. *J. Phys. Chem. C*, **2014**, *118*, 8445-8454. doi:10.1021/jp500931g
- 11 Gallaba, D. H.; Albesa, A. G. Migone, A. D. *J. Phys. Chem. C*, **2016**, *120*, 16649-16657. doi:10.1021/acs.jpcc.6b03481
- 12 Tanaka, S.; Fujita, K.; Miyake, Y.; Miyamoto, M.; Hasegawa, Y.; Makino, T.; Van der Perre, S.; Cousin Saint Remi, J.; Van Assche, T.; Baron, G. V. Denayer, J. F. M. *J. Phys. Chem. C*, **2015**, *119*, 28430-28439. doi:10.1021/acs.jpcc.5b09520
- 13 Zhang, C.; Gee, J. A.; Sholl, D. S. Lively, R. P. *J. Phys. Chem. C*, **2014**, *118*, 20727-20733. doi:10.1021/jp5081466

- 14 Yang, F.; Mu, H.; Wang, C.; Xiang, L.; Yao, K. X.; Liu, L.; Yang, Y.; Han, Y.; Li, Y. Pan, Y. *Chem. Mater.*, **2018**, *30*, 3467-3473. doi:10.1021/acs.chemmater.8b01073
- 15 Cheng, X.; Zhang, A.; Hou, K.; Liu, M.; Wang, Y.; Song, C.; Zhang, G. Guo, X. *Dalton Trans.*, **2013**, *42*, 13698-13705. doi:10.1039/C3DT51322J
- 16 Kundu, T.; Wahiduzzaman, M.; Shah, B. B.; Maurin, G. Zhao, D. *Angew. Chem. Int. Ed.*, **2019**, *58*, 8073-8077. doi:10.1002/anie.201902738
- 17 Kavoosi, N.; Bon, V.; Senkovska, I.; Krause, S.; Atzori, C.; Bonino, F.; Pallmann, J.; Paasch, S.; Brunner, E. Kaskel, S. *Dalton Transactions*, **2017**. doi:10.1039/C7DT00015D
- 18 Miura, H.; Bon, V.; Senkovska, I.; Ehrling, S.; Watanabe, S.; Ohba, M. Kaskel, S. *Dalton Trans.*, **2017**, *46*, 14002-14011. doi:10.1039/C7DT02809A
- 19 Sakata, Y.; Furukawa, S.; Kondo, M.; Hirai, K.; Horike, N.; Takashima, Y.; Uehara, H.; Louvain, N.; Meilikhov, M.; Tsuruoka, T.; Isoda, S.; Kosaka, W.; Sakata, O. Kitagawa, S. *Science*, **2013**, *339*, 193-196. doi:10.1126/science.1231451
- 20 Schaber, J.; Krause, S.; Paasch, S.; Senkovska, I.; Bon, V.; Töbrens, D. M.; Wallacher, D.; Kaskel, S. Brunner, E. *J. Phys. Chem. C*, **2017**, *121*, 5195-5200. doi:10.1021/acs.jpcc.7b01204
- 21 Férey, G. Serre, C. *Chem. Soc. Rev.*, **2009**, *38*, 1380-1399. doi:10.1039/B804302G
- 22 Millange, F.; Serre, C. Férey, G. *Chem. Commun.*, **2002**, 822-823. doi:10.1039/B201381A
- 23 Krause, S.; Bon, V.; Stoeck, U.; Senkovska, I.; Töbrens, D. M.; Wallacher, D. Kaskel, S. *Angew. Chem. Int. Ed.*, **2017**, *56*, 10676-10680. doi:10.1002/anie.201702357
- 24 Shi, Y.-X.; Li, W.-X.; Zhang, W.-H. Lang, J.-P. *Inorg. Chem.*, **2018**, *57*, 8627-8633. doi:10.1021/acs.inorgchem.8b01408
- 25 Su, J.; Yuan, S.; Wang, H.-Y.; Huang, L.; Ge, J.-Y.; Joseph, E.; Qin, J.; Cagin, T.; Zuo, J.-L. Zhou, H.-C. *Nat. Commun.*, **2017**, *8*, 2008. doi:10.1038/s41467-017-02256-y
- 26 Li, X.; Chen, X.; Jiang, F.; Chen, L.; Lu, S.; Chen, Q.; Wu, M.; Yuan, D. Hong, M. *Chem. Commun.*, **2016**, *52*, 2277-2280. doi:10.1039/C5CC09461E
- 27 Maji, T. K.; Mostafa, G.; Matsuda, R. Kitagawa, S. *J. Am. Chem. Soc.*, **2005**, *127*, 17152-17153. doi:10.1021/ja0561439
- 28 Tanaka, D.; Nakagawa, K.; Higuchi, M.; Horike, S.; Kubota, Y.; Kobayashi, T. C.; Takata, M. Kitagawa, S. *Angew. Chem. Int. Ed.*, **2008**, *47*, 3914-3918. doi:10.1002/anie.200705822
- 29 Bon, V.; Kavoosi, N.; Senkovska, I. Kaskel, S. *ACS Appl. Mater. Interfaces*, **2015**, *7*, 22292-22300. doi:10.1021/acsami.5b05456
- 30 Schaate, A.; Roy, P.; Godt, A.; Lippke, J.; Waltz, F.; Wiebcke, M. Behrens, P. *Chem. Eur. J.*, **2011**, *17*, 6643-6651. doi:10.1002/chem.201003211
- 31 Morris, W.; Wang, S.; Cho, D.; Auyeung, E.; Li, P.; Farha, O. K. Mirkin, C. A. *ACS Appl. Mater. Interfaces*, **2017**, *9*, 33413-33418. doi:10.1021/acsami.7b01040
- 32 Hu, Z.; Castano, I.; Wang, S.; Wang, Y.; Peng, Y.; Qian, Y.; Chi, C.; Wang, X. Zhao, D. *Cryst. Growth Des.*, **2016**, *16*, 2295-2301. doi:10.1021/acs.cgd.6b00076
- 33 Zahn, G.; Schulze, H. A.; Lippke, J.; König, S.; Sazama, U.; Fröba, M. Behrens, P. *Microporous Mesoporous Mat.*, **2015**, *203*, 186-194. doi:10.1016/j.micromeso.2014.10.034
- 34 Bueken, B.; Van Velthoven, N.; Willhammar, T.; Stassin, T.; Stassen, I.; Keen, D. A.; Baron, G. V.; Denayer, J. F. M.; Ameloot, R.; Bals, S.; De Vos, D. Bennett, T. D. *Chem. Sci.*, **2017**, *8*, 3939-3948. doi:10.1039/C6SC05602D
- 35 Liu, L.; Zhang, J.; Fang, H.; Chen, L. Su, C.-Y. *Chem. Asian J.*, **2016**, *11*, 2278-2283. doi:10.1002/asia.201600698
- 36 Liu, L.; Chen, Z.; Wang, J.; Zhang, D.; Zhu, Y.; Ling, S.; Huang, K.-W.; Belmabkhout, Y.; Adil, K.; Zhang, Y.; Slater, B.; Eddaoudi, M. Han, Y. *Nat. Chem.*, **2019**. doi:10.1038/s41557-019-0263-4
- 37 Øien, S.; Wragg, D.; Reinsch, H.; Svelle, S.; Bordiga, S.; Lamberti, C. Lillerud, K. P. *Cryst. Growth Des.*, **2014**, *14*, 5370-5372. doi:10.1021/cg501386j
- 38 Furukawa, H.; Gándara, F.; Zhang, Y.-B.; Jiang, J.; Queen, W. L.; Hudson, M. R. Yaghi, O. M. *J. Am. Chem. Soc.*, **2014**, *136*, 4369-4381. doi:10.1021/ja500330a
- 39 Kim, H.; Yang, S.; Rao, S. R.; Narayanan, S.; Kapustin, E. A.; Furukawa, H.; Umans, A. S.; Yaghi, O. M. Wang, E. N. *Science*, **2017**, *356*, 430-434. doi:10.1126/science.aam8743
- 40 Kim, H.; Rao, S. R.; Kapustin, E. A.; Zhao, L.; Yang, S.; Yaghi, O. M. Wang, E. N. *Nat. Commun.*, **2018**, *9*, 1191. doi:10.1038/s41467-018-03162-7
- 41 Kalmutzki, M. J.; Diercks, C. S. Yaghi, O. M. *Adv. Mater.*, **2018**, *30*, 1704304. doi:10.1002/adma.201704304
- 42 Simon, K.; Volodymyr, B.; Ulrich, S.; Irena, S.; M., T. D.; Dirk, W. Stefan, K. *Angew. Chem. Int. Ed.*, **2017**, *56*, 10676-10680. doi:10.1002/anie.201702357
- 43 Shivanna, M.; Yang, Q.-Y.; Bajpai, A.; Sen, S.; Hosono, N.; Kusaka, S.; Pham, T.; Forrest, K. A.; Space, B.; Kitagawa, S. Zaworotko, M. J. *Sci. Adv.*, **2018**, *4*. doi:10.1126/sciadv.aag1636
- 44 Zheng, B.; Fu, F.; Wang, L. L.; Wang, J.; Du, L. Du, H. *J. Phys. Chem. C*, **2018**, *122*, 4300-4306. doi:10.1021/acs.jpcc.7b10928
- 45 Thornton, A. W.; Babarao, R.; Jain, A.; Trouselet, F. Coudert, F. X. *Dalton Trans.*, **2016**, *45*, 4352-4359. doi:10.1039/C5DT04330A
- 46 Dissegna, S.; Vervoorts, P.; Hobday, C. L.; Düren, T.; Daisenberger, D.; Smith, A. J.; Fischer, R. A. Kieslich, G. *J. Am. Chem. Soc.*, **2018**. doi:10.1021/jacs.8b07098

